SIMULATED ABUNDANCES IN THE MASSIVE ECLIPSING BINARY STAR RY SCUTI

By

STEPHEN S. MCMILLAN

A thesis submitted in partial fulfillment of
the requirements for the degree of

MASTER OF SCIENCE

UNIVERSITY OF MINNESOTA
School of Physics and Astronomy

JUNE 2020

ACKNOWLEDGMENT

First I wish to express my most sincere appreciation to my Advisor Dr. Robert Gehrz. His guidance and words of advice were invaluable in the course of this research. Without his help, this work would never have been realized.

I must also acknowledge the support of my family and friends. My family's example has been a guiding light in my life. To my friends, I thank you for providing a little sanity and levity to my life. I would not have completed this work without those lighter moments.

Based in part on observations made with the NASA/DLR Stratospheric Observatory for Infrared Astronomy (SOFIA). SOFIA is jointly operated by the Universities Space Research Association, Inc. (USRA), under NASA contract NNA17BF53C, and the Deutsches SOFIA Institut (DSI) under DLR contract 50 OK 0901 to the University of Stuttgart.

SIMULATED ABUNDANCES IN THE MASSIVE ECLIPSING

BINARY STAR RY SCUTI

Abstract

by Stephen S. McMillan, M.Sc.
University of Minnesota
June 2020

Advisor: Robert D. Gehrz

Spectroscopic observations of the massive eclipsing binary RY Scuti and its double-ringed circumstellar nebula with the Stratospheric Observatory for Infrared Astronomy (SOFIA) were modeled using the *Cloudy* photoionization to determine the abundance of neon in the ionized gas torus. Line ratios were taken, and a best fit simulation was produced using chi-squared analysis as a measure of the goodness of fit. Using this best fit simulation, it was determined the neon to hydrogen ratio is overabundant with respect to solar levels by a factor of 5.3 ± 0.9. This value falls within the range of abundances previously determined for RY Scuti. Study of the abundances suggests hydrogen might be depleted in the system, further confirmation of the possibility that RY Scuti is a Wolf-Rayet progenitor.

TABLE OF CONTENTS

CHAPTER

APPENDIX

LIST OF TABLES

LIST OF FIGURES

Chapter One

Introduction

1.1 Analytical History of RY Scuti

RY Scuti (HD 169515) is a post main sequence massive eclipsing binary system a distance of 1.8 ± 0.1 kpc from Earth (Smith et al., 2002). Historically, RY Scuti has been of significant interest, providing the first direct observational evidence for the [Fe III] forbidden line transition previously theorized (Edlen and Swings, 1939). In addition to this historical significance, RY Scuti exhibits Roche lobe overflow, and has a toroidal double-ring nebula surrounding the stars themselves. This nebula has proven a most intriguing, and perplexing feature.

This double-ring nebula is discussed in great detail in numerous publications (Gehrz et al., 1995; Smith et al., 1999; Gehrz et al., 2001; Smith et al., 2011). Of primary interest is the observed [Ne II] forbidden line transition that occurs strongly in the inner ionized region of the torus (Gehrz et al., 2001), as this has allowed for the determination of the neon abundance in the region. Before this neon line is discussed in greater detail, a brief summary of the known physical characteristics of the RY Scuti system follows.

The primary star currently has a mass of 7.1 ± 1.2 $M_{\odot}$ and the secondary has a mass of 30.0 ± 2.1 $M_{\odot}$ (Grundstrom et al., 2007). As Giuricin and Mardirossian (1981), Antokhina and Cherepashchuk (1988), and others suggest, the primary star

has undergone significant mass transfer to the secondary star by way of Roche lobe overflow. From the light curves, the orbital period of the two bodies has been found to be approximately 11 days (Smith et al., 2002). The luminosity was found to be $\approx 3.4\text{x}10^6$ $L_\odot$. Additionally, an average mass-loss rate has been determined by Martino et al. (1992) to be (0.15 to 1.4)x10^{-4} $M_\odot$ yr^{-1} by way of radiation driven winds through the outer Lagrangian point. This mass loss alone does not adequately account for the size nor shape of the double-ring nebula.

A proper motion survey was done of RY Scuti's nebula which determined the star has experienced discrete outbursts of ejecta twice, at an interval of approximately 120 years (Smith et al., 2011). This study further estimates ages for mass-loss ejection of 250 years ago for the outer ring, and 130 years ago for the inner ring. Additionally, due to the similar geometry and structure, it appears the same mechanism was responsible for both ejections, further implying that this was a long lasting event. While this mass ejection has produced an interesting feature, it does not account for a large quantity of mass, implying the mass transfer process in RY Scuti from the primary to the secondary star is a largely conservative process (Smith et al., 2011).

1.2 Neon-II Abundance

The question of neon abundance is an important one for RY Scuti. It was suggested by Giuricin and Mardirossian (1981) that RY Scuti is in an uncommon evolutionary stage and exhibits some of the qualities of a Wolf-Rayet (WR) system. Wolf-Rayet stars are massive stars at a late stage in their evolution process. They are typified by large mass loss rates and hydrogen depletion. Further, Wolf-Rayet stars have been determined to exhibit an overabundance in neon compared to cosmic levels (Smith and Houck, 2005). As the nitrogen produced in the CNO cycle is converted to neon, and the processes that convert neon to magnesium are inefficient, leading to

an increased abundance in neon. Values for the cosmic abundance of neon are given by Nieva and Przybilla (2012) as $n_{\mathrm{Ne}}/n_{\mathrm{He}} = 10^{-2.9}$. For comparison, Lodders (2019) references a solar neon abundance of $n_{\mathrm{Ne}}/n_{\mathrm{He}} = 10^{-2.82}$ with respect to helium, and $n_{\mathrm{Ne}}/n_{\mathrm{H}} = 10^{-3.90}$ with respect to hydrogen. This change in abundance occurs over the course of several thousand years. Given this, it should not be a surprise that WR stars are overabundant in neon compared to cosmic levels, as neon is only created through stellar nucleosynthesis, with none produced in the big bang.

Further calculations for the neon abundances in a known WR star were done, yielding a value of more than ∼11 times the cosmic value, approaching the expected result of ∼18 times cosmic levels (Smith and Houck, 2005). Calculations for other stars that were earlier in their evolution were also done, and did not see a marked increase in the neon abundance, lending credence to the timescale mentioned above. Further study of RY Scuti has provided evidence to suggest the binary system is a WR progenitor (Antokhina and Cherepashchuk, 1988; Smith et al., 2002; Smith et al., 2011). As RY Scuti has been shown to exhibit the mass loss indicative of WR stars, an examination of the neon abundance would further cement this supposition.

The toroidal nebula around RY Scuti exhibits a strong [Ne II] forbidden line. Grasdalen et al. (1979) discussed a flux excess around the 10 μm range. With a greater spectral resolution, Gehrz et al. (1995) were able to resolve this excess as being due to a strong 10 μm silicate emission feature and a strong [Ne II] line at 12.8 μm. They then determined limits on the abundance of neon with respect to hydrogen to be (1.6 to 10)x$10^{-4} n_{\mathrm{Ne}}/n_{\mathrm{H}}$, or 1.6 to 10 times solar levels. This overabundance measurement was further improved upon by Gehrz et al. (2001) to be $n_{\mathrm{Ne}}/n_{\mathrm{H}} \geq 1.77\mathrm{x}10^{-4}$, or greater than 1.77 times solar abundance as stated by Holweger (2001). As previous studies of RY Scuti examine the abundances with respect to solar levels, it is convenient to discuss the abundances in this manner, as opposed to using cosmic levels as a point of comparison.

Using $\sim$5 μm to $\sim$36 μm spectra recently acquired with the Stratospheric Observatory for Infrared Astronomy (SOFIA), a series of simulations are done of the environment, and the resultant emission spectra is found for the double-ring nebula surrounding RY Scuti using spectral synthesis code *Cloudy* (Ferland et al., 2017). The goal of this simulation is to, in part, confirm the most recent calculations for the abundance of neon. In chapter 2, the new observations and reduction of those data will be discussed, followed by an overview of *Cloudy* in chapter 3. In chapter 4, the results of the simulations are presented. Chapter 5 will discuss the simulations, their results, as well as areas that can be improved upon for future analyses of both RY Scuti and similar systems using *Cloudy*.

Chapter Two

SOFIA Observations

2.1 Observations

The work herein utilizes data collected on the binary star RY Scuti on June 6$^{\text{th}}$, 2014 using the NASA Stratospheric Observatory for Infrared Astronomy (SOFIA; Young et al., 2012). The data were taken with the Faint Object Infrared Camera for the SOFIA Telescope (FORCAST; Herter et al., 2018), which is a mid-infrared spectrograph and camera. These particular data were taken with the four silicon grisms covering the wavelength ranges of 4.9 to 8.0 μm, 8.4 to 13.7 μm, 17.6 to 27.7 μm, and 28.7 to 37.1 μm. The integration times for each grism were 59.96 s, 287.79 s, 989.56 s, and 1752.76 s respectively. Of note is the gap in coverage between the second and third grisms. Atmospheric absorption that occurs above the flight level of SOFIA is present in roughly the 13.5 to 17.5 micron range. As such, the grisms are designed around this range, as can be seen in Fig 2.1. As will later be seen in Fig 4.1, there is a [Ne III] line present in this gap. The data were collected for PI Nathan Smith under PID 02_0101. These data were processed to level 3 using SOFIA standard stars through the SOFIA Science Center pipelines. This means the data have been flux calibrated, and a telluric correction has been applied.

The coverage of this mid-infrared region allows for the examination of the [Ne II] line at 12.8 μm. In addition, this spectral coverage provides several other reasonably

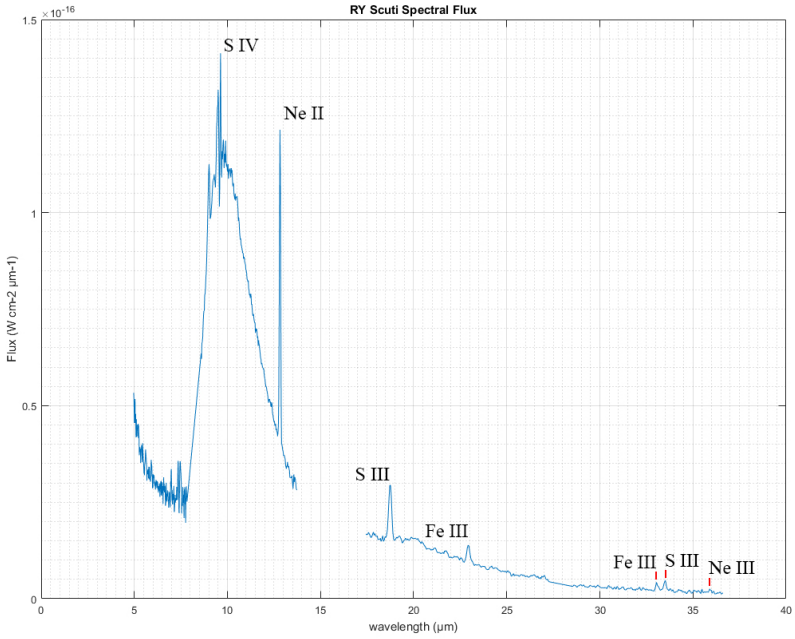

Figure 2.1 Observed emission spectrum from 5 to 36 μm. This image shows the experimental data taken on June 6$^{\text{th}}$, 2014. The individual lines that have been identified are labeled in the image. These lines are used as the basis of the fit parameters for the simulations as seen in Fig. 4.1.

strong metallic forbidden emission lines, including a pair of [Fe III] lines at 22.93 μm and 33.01 μm, which can be used as points of comparison. As can be seen in Fig. 2.1, this region also includes several sulfur lines in addition to the aforementioned [Fe III] lines and the neon line of note. As was mentioned previously, RY Scuti was the capstone for the [Fe III] forbidden emission line, so from a historical perspective, it is fitting they be used to aid in the examination of neon here.

Chapter Three

Cloudy

3.1 Background

In order to independently verify possible values for the neon abundance, it was decided that photoionization modeling of the emitting gas torus around RY Scuti would be an appropriate method. Photoionization modeling allows for the simulation of a spectral region, which can be used to create an output spectra, which in the case of RY Scuti can then be compared to the SOFIA data previously shown. Of the various simulation options available, *Cloudy* was chosen. *Cloudy* is a spectral synthesis suite first written by Gary J. Ferland in 1978. The work done here was completed using *Cloudy* C17.01, last described by Ferland et al. (2017). In addition to the download for *Cloudy* is a set of documents that describe how *Cloudy* works and can be used. These documents are aptly called *Hazy*, of which there are three in the series. *Hazy* 1 in particular has been of particular aid, as it describes the numerous commands available to the software. The other *Hazy* documents provide a discussion of the various outputs, and a discussion of the physics behind *Cloudy* respectively. The *Hazy* documents are again discussed by Ferland et al. (2017).

Cloudy has the capability of modeling complex systems, allowing for varied geometries, non-linear densities, varied radiation fields, and of course chemical compositions. The primary focus of the work has been in the chemical compositions, focusing on

elemental abundances. For a complete picture of the versatility of *Cloudy*, a thorough examination of *Hazy* would be in order. As will be discussed in the next chapter, the simulation of RY Scuti was done with several assumptions.

3.2 Basic Commands

The following are basic definitions of the commands used for simulating RY Scuti. How and why these commands were used will be discussed in greater detail in Chapter 4. For many of the commands below several distinct options were available in *Cloudy*, including in most cases a choice of units, and in using different geometric models.

- **title** - Allows for organization of results, and has no bearing on how the simulation is run.
- **blackbody** - Sets the relative blackbody temperature of the source star in K.
- **luminosity** - Scales the luminosity of the source star, given as the log of the luminosity in erg/s. Other units can be used.
- **radius** - Sets the radius of emission region, by default in units of the log of the radius in cm.
- **hden** - Sets the base hydrogen density. For the case of RY Scuti, this primarily serves to scale the observed lines.
- **sphere** - Sets the simulation to assume a spherical geometry.
- **abundances** - Sets the abundance of each element in terms of the log of the ratio compared to hydrogen. It is important to note that *Cloudy* does not read the element name, but rather the order of the elements. To that end, every element shown in Fig. B.1 must be included in the exact order, even if a particular element isn't to be varied.

In addition to these commands, others were used to force multiple iterations, and to save the output as several different file types. The first saves the output continuum in a delimited text file. The results were additionally output as a FITS file, giving another option for analysis. As the emission lines proved to be the main focus of the research, nothing was done with the FITS files, but there may be other ways FITS could be utilized in future research.

Chapter Four

Simulations and Results

4.1 The Simulations

The simulations in *Cloudy* were designed with the intention of finding a set of input variables that would reproduce the observed line strength ratios from the collection of data from SOFIA. To that end, the inputs were initially set to solar elemental abundances as a baseline. As expected, these results were significantly divergent from the observed line ratios. As the data set contains only a handful of lines in the families of sulfur, iron and neon, those specific elements were chosen to be adjusted, leaving the others at solar defaults.

Outside of the abundances, several key assumptions were made for the majority of the simulations. As to the geometry of the nebula, both cylindrical and spherical geometries were tested. More on the geometries is discussed later in the chapter. Additionally, the density of the nebula was assumed to be uniform.

The continuum emission in the 5-30 μm range originates from a different spatial region than is occupied by the ionized gas in which the free-free and forbidden line emissions arise. However, Gehrz et al. (1995), find the free-free contribution to the continuum in this spectral region is significantly less than one percent. As such, in order to compare the simulated and observed spectra, it was decided a comparison of the line ratios would suffice. The line ratios should remain the same with the

caveat that the lines being compared to each other need to be within a fairly short range in wavelength. Even though other spectral ranges have been taken of RY Scuti, none could be effectively utilized in addition to the SOFIA data used here, without a rescaling based on the functional form of the free-free emission. For this research, just the one spectral range was used.

With the *Cloudy* input set to solar elemental abundances, each simulation changed only one elemental input at a time, starting with sulfur and iron, leaving the neon abundance for last. While the first round of fitting was done by eye until the ratios were reasonably close to the observed values, a chi-squared analysis was done for each simulation thereafter. As the fits grew closer to the observed line ratios and the corresponding chi-squared values dropped, the simulations would continue to be adjusted until the fit grew worse again. At this point, the abundance value for the particular line was returned to the best observed value. This process was then repeated for the other elements being varied. This process was repeated in sets of three until the changes being made in each run were having little to no effect on the calculated value of the reduced chi-squared. An improvement on this process will be discussed in the next chapter.

In total, more than 100 different simulations were run through a remote access to a Linux machine, adjusting primarily the abundances of the above elements. As it stands, each simulation was performed, and the results analyzed through a Matlab script as described above. Suggested improvements to this technique will be discussed in detail in the next chapter.

A series of simulations were run in an attempt to more closely model the toroidal nature of the nebula surrounding RY Scuti using the cylindrical function built into *Cloudy*, as this function can allow for varying nebula radii, and heights. Numerous simulations were run using various cylindrical parameters, though none of the trials produced results that differed from the spherical simulations. As the spherical simula-

tions seemed less computationally intense, the remainder of the simulations were done with a spherical geometry. A test of a much lower hydrogen density was also run in an effort to model potential hydrogen depletion. In this case, the *Cloudy* simulation would not even run, citing conditions outside its normal operating parameters.

4.2 Results

This section will examine the output from *Cloudy* for the best fit determined by the methodology discussed above. While several dozen more simulations were run after this particular trial, none fared better at replicating the line ratios. Figure A.1 shows the inputs used in *Cloudy* to arrive at the resultant spectral emission lines.

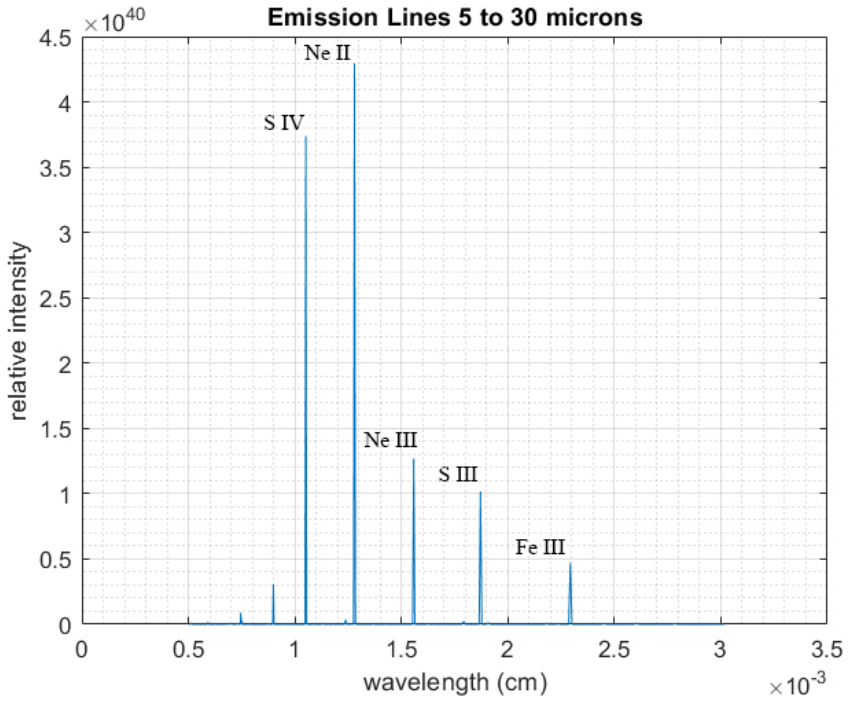

Figure 4.1 Simulated Emission Spectrum from 5 to 36 μm. This image shows the simulated spectral results from *Cloudy* for the best fit simulation. At the scales output from *Cloudy*, the tail end of the region is difficult to see. As such, a zoomed in segment can be seen in Fig. 4.2. The line that can be seen at 15.58 μm is a Ne III line, but as that region in the experimental data is absent, that line will not be studied here.

The output spectra, as seen in Fig. 4.1, show the same range as the SOFIA data in Fig. 2.1. As was mentioned previously, the wavelength gap between the second and third grisms created a gap in the data. This gap is clearly not present in the simulated spectra, and as can be seen, there is a [Ne III] line present at $\lambda = 15.58$ μm. Based on the simulations, this neon line should have a relative strength that is greater than the sulfur line adjacent to it.

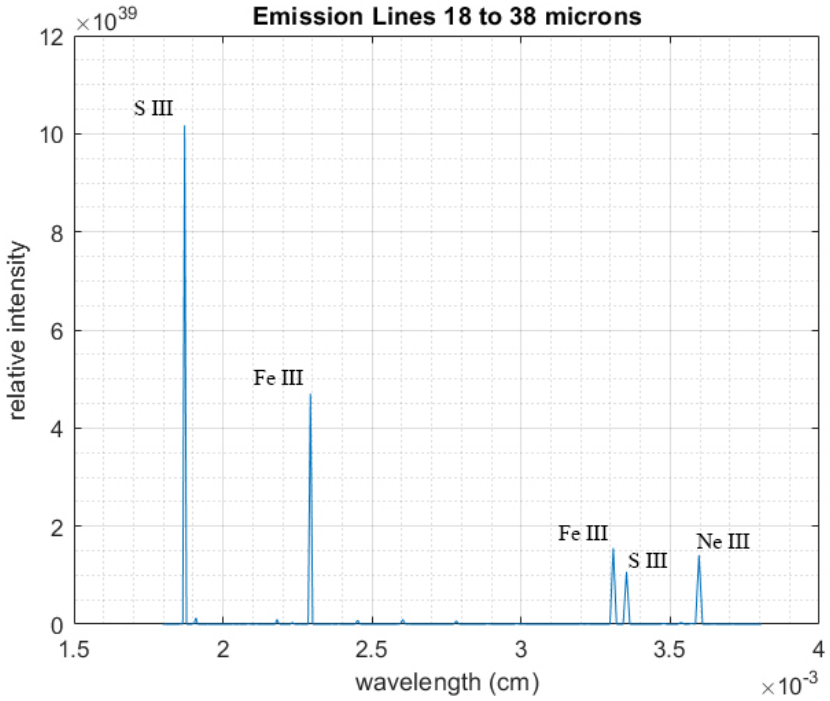

Figure 4.2 Simulated Emission Spectrum from 18 to 36 μm. This image shows a scaled version of Fig. 4.1. Here we can better see the tail end of the region in question. It does contain the lines we expect to see from the data, though the Ne III line and the Fe III line are stronger than expected compared to the data as seen in Fig. 2.1. There are some possible fixes in the code for this that will be discussed later.

As the line strengths drop precipitously in scale, the tail end of the range in question becomes difficult to see. Figure 4.2 shows a re-scaled version of this section of the plot. While the plot from the data has the [S III] line dominating the [Fe III] line, the best fit simulation shows the opposite. The difference between these lines

does fall close to the flux uncertainty in the SOFIA data, however from the ionization potential of these two lines, it should be expected that [S III] should dominate the [Fe III] line. A possible explanation for this disparity will be discussed in chapter 5.

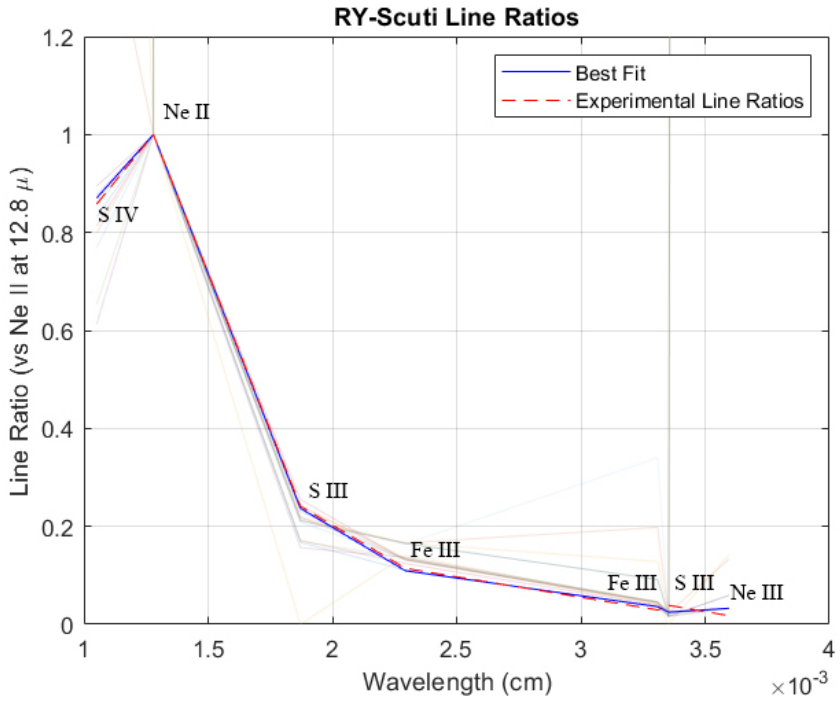

Figure 4.3 RY Scuti Simulated Line Ratios. This image shows a variety of the simulations that were run in order to narrow down a best fit in the elemental abundances for RY Scuti. The best fit simulation shown in the solid blue line yielded a reduced chi-squared value of $\chi^2_{red} = 1.28$. Each line as shown in Fig. 4.1 was taken in ratio to the Ne II lines, and compared to the same ratios from the experimental data as seen in Fig. 2.1.

With the line intensities calculated using *Cloudy*, the line ratios are then easily calculated. Neon was used as the point of comparison, as it contains the strongest line in the region. In order to get the best visualize the data, the line ratios were plotted against their wavelengths, as can be seen in Fig. 4.3. As can also be seen, the observed line ratios from the SOFIA data are plotted as a red dashed line. A variety, but not all of, the completed simulations are represented in this figure. The best fit line in blue is the simulation run that produced the minimal value during the

chi-squared analysis.

As for the last several microns of the spectral range, the iron and neon ratios appear to be a little high, and the sulfur a little low. However as the sulfur line at $\lambda = 18.7$ μm very closely matches the observed line ratio, as does the iron line at $\lambda = 22.9$ μm, it is reasonable to conclude that there may be other factors involved in these lines that were not taken into account in the simulations herein. Potential factors will be explored in the next chapter.

4.3 Error Analysis

As was previously mentioned, a chi-squared analysis was performed for each simulation by the following equation:

$$\chi^2 = \sum_{i=1}^{N} \frac{(O_i - E_i)^2}{{\sigma_i}^2} \tag{4.1}$$

where O_i is the simulated line ratio, E_i is the observed line ratio, and σ is the variance in each line ratio, which is based on the spectral flux error from the SOFIA data. The sum ranges over the line ratios measured in each simulation. Further, a value for the reduced chi-squared was calculated by:

$$\chi^2_{red} = \frac{\chi^2}{N - p} \tag{4.2}$$

where N is again the number of line ratios being tested, and p is the number of fit parameters. In this case, there are six lines as points of comparison, and three parameters being fit.

For the best fit simulation, a reduced chi-squared was determined to be 1.28. From a statistical perspective, the optimal value of the reduced chi-squared is around one. The reduced chi squared here larger than one implies that the simulations have not fully captured the realities of the emission region in RY Scuti.

Each of the abundances were varied in turn until the changes produced a worse chi-squared result. Determination of the error in the simulated values was accomplished by examining the range of values lying withing approximately one standard deviation of the minima for each parameter. This yielded values of the log of the line ratio compared to hydrogen of -3.28 ± 0.8, -3.94 ± 0.8, and -3.38 ± 0.5 for each neon, sulfur and iron respectively.

As a direct comparison to solar ratios is convenient in this case, the uncertainty was propagated by the following:

$$\delta f = 10^x \ \log x \ \delta x \tag{4.3}$$

This yields the error for the non-logarithmic expression of the line ratios. It should be noted that with such few points used for the chi-squared analysis for each simulation, the fit process would benefit from examining a greater number of line ratios. Further improvements on this technique will be discussed in the next chapter.

Chapter Five

Discussion and Conclusions

5.1 Discussion

Cloudy proved to have a fairly high learning curve, but after several long weeks of becoming familiar with the system and its intricacies, further simulations would be reasonably simple. As for this sort of simulation, *Cloudy* excelled, proving quite capable of creating emission spectra based on provided inputs.

For further studies of RY Scuti using *Cloudy*, there are several areas that could be focused on. The first of which is the test of various geometries. *Cloudy* has the capability of handling a variety of inputs, including inner and outer radii, covering factors, illuminated faces, and expanding structure. Further, options to include ionization factors are available in *Cloudy*. The nebula around RY Scuti is ionized, which could provide a change to some of the lines in question. These, and many more, options could prove useful in further simulations.

As was previously discussed, the fitting of the line ratios was done with a chi-squared analysis. A much more robust technique would see a full least squares fit done, though even with three fit parameters, such work would prove incredibly time consuming. One possibility of improving on this technique includes work by Vanlandingham (1998) using software MINUIT, originally described by James and Roos (1975). MINUIT is a numerical minimization routine which would allow for simplified

least squares fitting. Using this technique, it is reasonable to assume a better fit, of more of the fundamental parameters, could be accomplished. Not only would this allow for fitting of the abundances, but it could allow for variation in the geometry, and other input variables. This would go a long way to confirming the validity of these techniques for RY Scuti.

MINUIT itself need not be used if access is had to another such fitting program that can allow for the change of an input file, and the running of further simulations between each fitting attempt. This adjustment would allow for confirmation of some of the variables discussed in chapter 1, including temperature, luminosity, and hydrogen density. These, in addition to the various geometries previously mentioned, should provide significantly higher confidence in the overabundances seen in the nebula.

Further simulations are also warranted to examine other ranges of wavelength. Many spectra have been taken of RY Scuti over the years, and some previous work has been done in describing the line strengths of note (Smith et al., 2002).

5.2 Conclusion

After completing the iterative simulation process using *Cloudy* for the toroidal nebula surrounding RY Scuti, the abundances of note have been determined as is shown below in Table 5.1.

Element	log(n/n(H))	n/n(H)	Ratio vs Solar Values
Ne	-3.28 ± 0.08	(5.3 ± 0.9)E-04	5.3 ± 0.9
S	-3.94 ± 0.08	(1.2 ± 0.2)E-04	6.6 ± 1.1
Fe	-3.38 ± 0.05	(4.2 ± 0.5)E-04	14.9 ± 1.8

Table 5.1 This tables shows the simulated results for the best fit as seen in Fig. 4.3.

As can be seen from Table 5.1, the abundances used for the best fit give a neon

abundance compared to solar levels of 5.3 ± 0.4. This is a promising result as it lies within the range of values as stated by Gehrz et al. (1995). We additionally see that the levels of both sulfur and iron appear to be elevated well above normal solar levels.

As RY Scuti is a post-main-sequence massive binary, it is not unreasonable to see a higher amount of iron, sulfur and neon in the nebula of the stars' ejecta, as each of these elements is a byproduct of fusion reactions that occur in massive stars. However, considering there is such a large increase in the abundance ratios here, this seems to suggest that RY Scuti is perhaps much depleted in hydrogen. This would certainly skew the ratios of each of the elements to a higher value. This further supports the conjecture that RY Scuti is a progenitor to a Wolf-Rayet star (Smith et al., 2011).

REFERENCES

Antokhina, E. A. and A. M. Cherepashchuk (1988). "RY-Scuti as a Progenitor of a WR+OB System". In: *Soviet Astronomy Letters* 14 (NO.2), p. 105.

Edlen, B. and P. Swings (1939). "Forbidden FeIII-lines in Celestial Spectra". In: *The Observatory* 62, pp. 234–235.

Ferland, G. J. et al. (2017). "The 2017 Release of Cloudy". In: *Revista Mexicana de Astronomia y Astrofisica* 53, pp. 385–438.

Gehrz, R. D. et al. (1995). "RY Scuti: Infrared and Radio Observations of the Mass-Loss Wind of a Massive Binary Star System". In: *The Astrophysical Journal* 439, pp. 417–430.

Gehrz, R. D. et al. (2001). "KECK LWS Images of the Compact Nebula Around RY Scuti in the Thermal Infrared". In: *The Astrophysical Journal* 559, pp. 395–401.

Giuricin, G. and F. Mardirossian (1981). "A lightcurve analysis for the massive binary RY Sct." In: *Astronomy and Astrophysics* 101, pp. 138–141.

Grasdalen, G. L. et al. (1979). "RY Scuti: Silicates Around an Early-Type Supergiant Binary System". In: *The Astrophysical Journal* 234, pp. 129–133.

Grundstrom, Erika D. et al. (2007). "A Spectroscopic Study of Mass Outflows in the Interacting Binary RY Scuti". In: *The Astrophysical Journal* 667, pp. 505–519.

Herter, T.L. et al. (2018). "FORCAST: A Mid-Infrared Camera for SOFIA". In: *Journal of Astronomical Instrumentation* 07 (04).

Holweger, H. (2001). "Photospheric abundances: Problems, updates implications". In: *A Joint SOHO/ACE Workshop. AIP Conference Proceedings* 598, p. 23.

James, F. and M. Roos (1975). "MINUIT - A System for Function Minimization and Analysis of the Parameter Errors and Correlations". In: *Computer Physics Communications* 10 (6), pp. 343–367.

Lodders, Katharina (2019). "Solar Elemental Abundances". In: *The Oxford Research Encyclopedia of Planetary Science*.

Martino, D. de et al. (1992). "High Resolution Spectroscopic Observations of the Massive Binary RY Scuti". In: *Astronomy and Astrophysics* 254, pp. 266–273.

Nieva, M.F. and N. Przybilla (2012). "Present-day cosmic abundances. A comprehensive study of nearby early B-type stars and implications for stellar and Galactic evolution and interstellar dust models". In: *Astronomy & Astrophysics* 539, p. 57.

Smith, J. and James R. Houck (2005). "The Neon Abundance of Galactic Wolf-Rayet Stars". In: *The Astrophysical Journal* 622 (2), pp. 1044–1051.

Smith, N. et al. (1999). "Hubble Space Telescope Images of the Compact Nebula Around RY Scuti". In: *The Astrophysical Journal* 118, pp. 960–971.

— (2002). "The WR+OB Progenitor RY Scuti: Intensive Spectroscopy of Its Compact Double-Ring Nebula". In: *The Astrophysical Journal* 578, pp. 464–485.

— (2011). "Episodic mass loss in binary evolution to the Wolf-Rayet phase: Keck and HST proper motions of RY Scuti's nebula". In: *Monthly Notices of the Royal Astronomical Society* 418.3, pp. 1959–1972.

Vanlandingham, K. M. (1998). "Optimization Methods in Nebular Analyses of Nova Ejecta". In: *ASP Conference Series* 137.

Young, E. T. et al. (2012). "Early Science with SOFIA, the Stratospheric Observatory For Infrared Astronomy". In: *The Astrophysics Journal Letters* 749 (02).

APPENDIX

Appendix A

```
*************************************17Jun01*************************************
*                                                                              *
* title H II Region                                                            *
* blackbody 4.0e4 K                                                            *
* luminosity total 40.28                                                       *
* radius 16.35                                                                 *
* hden 5                                                                       *
* sphere                                                                       *
* abundances he=-1 li=-8.69 be=-10.58 b=-9.21 c=-3.61 n=-4.07 o=-3.31          *
* continue   f=-7.52 ne=-3.275 na=-5.67 mg=-4.46 al=-5.53 si=-4.46 p=-6.5      *
* continue   s=-3.935 cl=-6.72 ar=-5.6 k=-6.88 ca=-5.64 sc=-8.83 ti=-7         *
* continue   v=-8 cr=-6.3 mn=-6.5 fe=-3.375 co=-7 ni=-5.8 cu=-7.8 zn=-7.4      *
* iterate                                                                      *
* Print last                                                                   *
* save continuum units cm "scuti.con"                                          *
* save FITS "scuti.fits"                                                       *
*                                                                              *
********************************************************************************
```

Figure A.1 Best Fit CLOUDY Input Code. This image shows the input commands for the best fit simulation as seen in Fig. 4.1. Of particular note are the abundance values (given in terms of the log of the ratio versus hydrogen) for neon at -3.275, for sulfur at -3.935, and iron at -3.375.

Appendix B

Order	Symbol	Element	log(n/n(H))
2	He	Helium	-1.00
3	Li	Lithium	-8.69
4	Be	Beryllium	-10.58
5	B	Boron	-9.21
6	C	Carbon	-3.61
7	N	Nitrogen	-4.07
8	O	Oxygen	-3.31
9	F	Fluorine	-7.52
10	Ne	Neon	-4.00
11	Na	Sodium	-5.67
12	Mg	Magnesium	-4.46
13	Al	Aluminum	-5.53
14	Si	Silicon	-4.46
15	P	Phosphorus	-6.50
16	S	Sulphur	-4.74
17	Cl	Chlorine	-6.72
18	Ar	Argon	-5.60
19	K	Potassium	-6.88
20	Ca	Calcium	-5.64
21	Sc	Scandium	-8.83
22	Ti	Titanium	-6.98
23	V	Vanadium	-8.00
24	Cr	Chromium	-6.33
25	Mn	Manganese	-6.54
26	Fe	Iron	-4.55
27	Co	Cobalt	-7.08
28	Ni	Nickel	-5.75
29	Cu	Copper	-7.79
30	Zn	Zinc	-7.40

Table B.1 This table shows the abundances and specific order in which to enter them for CLOUDY. These values were included in the Cloudy C17.01 documentation Hazy 1 as described by Ferland et al., 2017.